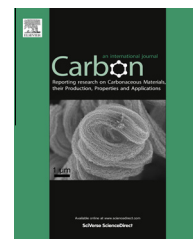


Available at www.sciencedirect.com

ScienceDirect

journal homepage: www.elsevier.com/locate/carbon

Controllable viscoelastic behavior of vertically aligned carbon nanotube arrays

Kilho Eom ^a, Kihwan Nam ^b, Huihun Jung ^b, Pilhan Kim ^c, Michael S. Strano ^d,
Jae-Hee Han ^{e,*}, Taeyun Kwon ^{c,*}

^a Biomechanics Laboratory, College of Sport Science, Sungkyunkwan University, Suwon 440-746, Republic of Korea

^b Department of Biomedical Engineering, Yonsei University, Wonju 220-710, Republic of Korea

^c Graduate School of Nanoscience and Technology, Korea Advanced Institute of Science and Technology (KAIST), Daejeon 305-701, Republic of Korea

^d Department of Chemical Engineering, Massachusetts Institute of Technology, Cambridge, MA 02139, USA

^e Department of Energy IT, Gachon University, Gyeonggi-do 461-701, Republic of Korea

ARTICLE INFO

Article history:

Received 9 May 2013

Accepted 18 August 2013

Available online 29 August 2013

ABSTRACT

We have characterized the mechanical behavior of aligned carbon nanotube (CNT) arrays that serve as foam-like energy absorbing materials, by using atomic force microscope indentation. It is shown that the mechanical properties (e.g. elastic modulus, adhesion force, and energy dissipation) of aligned CNT arrays are dependent on the length of CNTs as well as chemical environment that surrounds CNT arrays. More remarkably, it is found that CNT array made of CNTs with their length of 10 μm exhibits the excellent damping property (i.e. energy dissipation) higher than that of a conventional composite such as Kevlar. It is also shown that the energy dissipation of CNT arrays during loading–unloading process can be reduced by the solution surrounding CNT array, and that the decrease of energy dissipation for CNT array due to solution depends on the solution type, which mediates the interaction between individual nanotubes. Our study sheds light on the design principles for CNT array-based foam-like materials.

© 2013 Elsevier Ltd. All rights reserved.

1. Introduction

Carbon nanotube (CNT) has recently been considered as an excellent candidate for building blocks [1] for the development of large-scale hierarchical structures, which can serve as a multifunctional devices (e.g. antenna [2], resonator [3], etc.), due to the remarkable optical, electrical, and mechanical properties of CNT. For instance, it has been reported that CNT can possess the elastic modulus in the order of 1 TPa much higher than that of conventional materials [4,5], suggesting that CNT is a useful building block for the development of a structure performing the mechanical functions. This remarkable elastic property of CNT has led researchers

[6–9] to develop the vertically aligned CNT array that can serve as a foam-like material due to the viscoelastic behavior of CNT array. Specifically, when the aligned CNT array is mechanically compressed, the frictional interaction between individual CNTs driven by buckling of CNTs leads to the viscoelastic behavior of CNT array rather than the elastic deformation. When CNT array is compressed by mechanical force, CNT array absorbs the thermal energy during the deformation. On the other hand, when the mechanically compressed CNT array is released by unloading, CNT array dissipates the absorbed thermal energy. This observation suggests that CNT array can serve as a material that is capable of energy absorption and mechanical damping [9,10], which implies

* Corresponding authors.

E-mail addresses: jhhan388@gachon.ac.kr (J.-H. Han), taeyunkwon@kaist.ac.kr (T. Kwon).

0008-6223/\$ - see front matter © 2013 Elsevier Ltd. All rights reserved.

<http://dx.doi.org/10.1016/j.carbon.2013.08.030>

that CNT array can serve as an energy absorbing material that can be employed for engineering applications such as bullet-proof material in military. Until recently, a polymeric material such as Kevlar has been widely utilized as a damping material, due to its viscoelastic properties, that has been used for bullet-proof material in military. It is conjectured that CNT array may supersede the polymeric material due to the controllable viscoelastic properties of the CNT array as described in this work.

To characterize the mechanical behavior of CNT array in response to compression, we have employed atomic force microscope (AFM) indentation [11,12], which is useful in studying the mechanical behavior of nanoscale materials ranging from biological materials (e.g. virus [13], cell [14], etc.) to nanomaterial (e.g. CNT [15,16], nanowire [17–19], CNT membrane [20,21], etc.). For instance, the mechanical properties of nanomaterials can be extracted from AFM indentation experiments along with theoretical models. In particular, if the nanomaterial exhibits the elastic properties, the force–displacement curve obtained from AFM indentation can be fitted to Hertz theory [22] for extracting the elastic modulus of such nanomaterial. When the nanomaterial possesses the viscoelastic properties (as in the case of aligned CNT array [7]), Oliver–Pharr model [23] is suitable to extract the mechanical properties from the force–displacement curve obtained from AFM indentation.

Even though the mechanical behavior of aligned CNT array in response to mechanical compression has recently been extensively studied [6–8,10], it has been still not well studied how to optimize the mechanical (damping) properties of CNT array. In order for CNT array to act as an energy absorbing material and/or a mechanical damper [10], it is of high importance to know how to maximize the damping properties (i.e. energy dissipation) of CNT array, which has been rarely taken into account. Since the damping properties of CNT array originates from buckling-driven frictional interactions between CNTs during compression, it may be possible to optimize the damping properties of aligned CNT array through controlling the frictional interaction between individual CNTs. In this study, we have demonstrated how to achieve the optimized damping properties of aligned CNT array, which can serve as a foam-like material, based on controlling frictional interaction that depends on both the structural parameter of CNT array and the medium that surrounds CNT array.

2. Experimental

2.1. Preparation of aligned CNT array

For fabrication of aligned CNT array, we have utilized a conventional thermal-chemical-vapor-deposition (TCVD) system (SciEn Tech Co., Ltd.) that enables the chemical synthesis of aligned CNT array. The mechanisms of TCVD-based synthesis of CNT array are well described in a literature [24]. The TCVD system includes (i) hydrocarbon feedstock gas (ethylene, C₂H₄, 99.9%) as a carbon source, (ii) both hydrogen (H₂, 99.999%) and argon (Ar, 99.999%) gases as dilution and catalytic gases, and (iii) substrate on which iron (Fe) as a catalyst was deposited. In particular, the substrate consists of a p-type

silicon (100) wafer with a 3.5 μm layer of thermal SiO₂, where Fe catalyst with its thickness of 1 nm is deposited on a Al₂O₃ film with its thickness of 10 nm using an electron-beam evaporation method in a vacuum. The flow rate ratio of H₂ to C₂H₄ was maintained as approximately 2.5 during the growth stage, while the flow rate of Ar is given as 100 sccm. The growth time was varied in order to obtain CNT array whose length ranges between 1 and 10 μm. The chemical growth of CNTs was performed at 750 °C and atmospheric pressure. After the growth of CNT array, Ar gas was injected to TCVD system in order to cool the TCVD system to a room temperature. The synthesized CNT array was imaged using scanning electron microscopy (SEM, Hitachi S-4700) and transmission electron microscopy (TEM, TECNAI G2 F30 S-TWIN) as shown in Fig. 1a and b.

2.2. Nanomechanical indentation of CNT array

Fig. 1c illustrates the AFM-based indentation experiment that probes the mechanical behavior of CNT array in response to mechanical compression. Our conjecture is that the mechanical behavior of CNT array is well reflected into a force–displacement curve obtained from AFM indentation. In particular, if CNT array exhibits the elastic properties for the case in which friction between individual CNTs due to their buckling is unlikely to occur, then the force–displacement curve has a feature that the loading and unloading curves become identical to each other (Fig. 1d). On the other hand, if individual CNTs are buckled so as to induce the friction between CNTs during the compression of CNT array, then the force–displacement curve possesses a hysteresis loop, which is an indicative of the viscoelastic behavior. During the loading path, the mechanical compression leads CNT array to absorb thermal energy; on the other hand, during the unloading path, the mechanical relaxation of CNT array results in dissipating the absorbed energy. As previously reported in a literature [7], CNT array can exhibit the stress-relaxation behavior in response to static compressive strain, which is a signature of viscoelastic property.

3. Results

3.1. Role of CNT length on the mechanical behavior of CNT array

We have studied the effect of CNT length on the mechanical properties of CNT array, since the buckling of individual CNTs during the compression of CNT array is determined by the length of individual CNT. As shown in Fig. 2a, the force–displacement curve of CNT array consisting of short CNT (i.e. with its length of 1 μm) does not exhibit any hysteresis loop in the force–displacement curve, indicating that a mechanical compression leads to the elastic deformation of CNT array. In other words, when a force even up to 25 μN is applied to compress the CNT array, the individual CNTs are unlikely to be buckled so that the compression cannot lead to the mechanical friction between individual CNTs (for details, see below). However, the mechanical behavior of CNT arrays consisting of longer CNTs (i.e. with their length of 5 or 10 μm) in re-

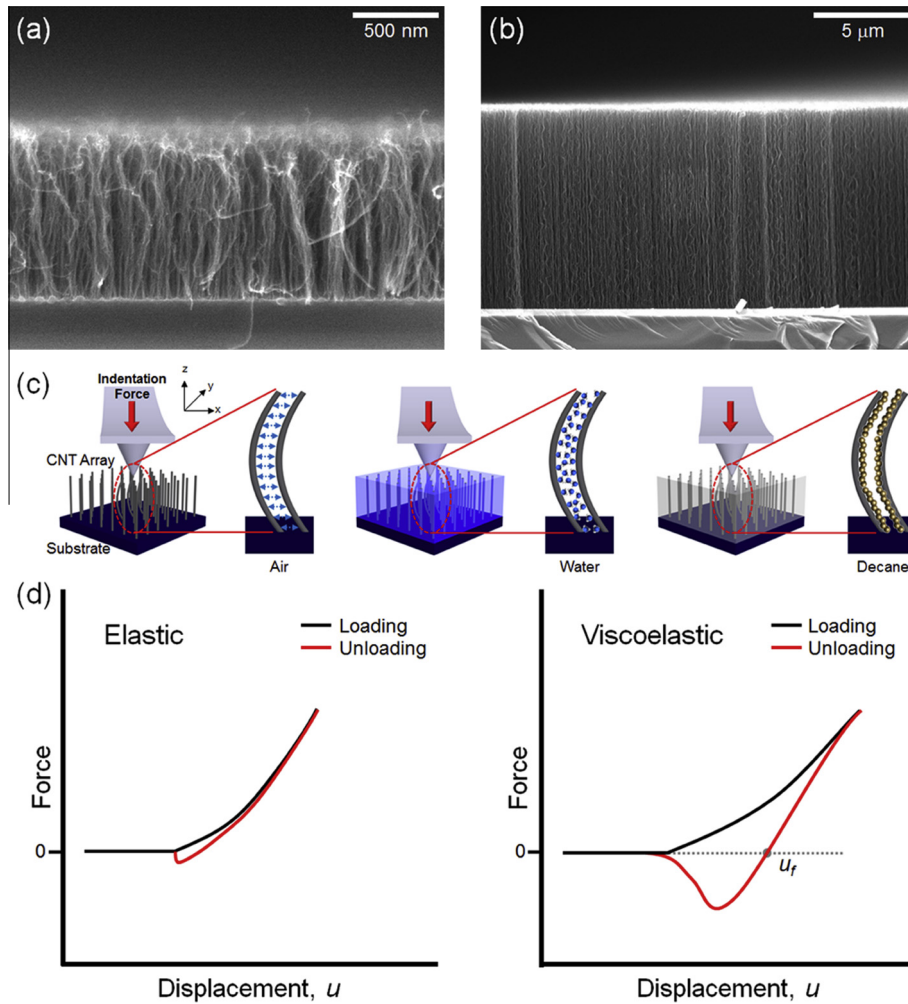


Fig. 1 – Schematic of nanomechanical indentation of aligned CNT array. Scanning electron microscope (SEM) images of CNT array with CNT length of (a) 1 μm or (b) 10 μm. (c) Nanomechanical indentation of CNT array surrounded by air [left panel], water [middle panel], or decane [right panel]. An enlarged inset of the schematic shows the mechanical frictions between two individual CNTs (that comprise CNT array) during indentation. (d) Mechanical behavior of CNT array: left panel shows the elastic behavior of CNT array, when individual CNTs do not undergo the mechanical frictions between them during the mechanical indentation. Right panel depicts the viscoelastic behavior of CNT array, when mechanical indentation induces the frictions between individual CNTs. (A colour version of this figure can be viewed online.)

sponse to a compressive force is quite different from that of CNT array composed of short CNTs. Specifically, the force–displacement curve of CNT array consisting of long CNTs in response to compression exhibits the hysteresis loop in the force–displacement curve, which is an indicative of viscoelastic properties. That is, the force of 25 μN is sufficient to induce the mechanical friction between CNTs during the compression of CNT array; such friction plays a critical role in the transition from elastic to viscoelastic behavior for CNT array.

For quantitative understanding the mechanical behavior of CNT array, we have considered the elastic beam theory, i.e. Euler–Bernoulli beam theory [25], that enables us to depict the buckling behavior of individual CNT. A critical stress that induces the buckling of CNT (responsible for the friction between individual CNTs) is represented in the form of $\sigma_{cr} = E_{CNT}(\pi r/L_{HW})^2$ (Ref. [6]), where E_{CNT} is the elastic modulus of CNT, r is the radius of CNT, and L_{HW} indicates the

half-wavelength of buckle along CNT. Accordingly, the critical force that results in the buckling of CNTs can be obtained as $F_{cr} = \sigma_{cr}A_{CNT}$, where A_{CNT} is the cross-sectional area of CNT. The critical force leading to the friction between CNTs with their length of 1 μm is computed as $F_{cr} = \sim 190 \mu\text{N}$, which is much larger than applied force (i.e. $F_{app} = 25 \mu\text{N}$). This suggests that an applied force of 25 μN is unable to induce the buckling of short CNTs so that the mechanical friction between CNTs is unlikely to occur. This implies that a mechanical compression due to force of 25 μN induces the elastic deformation of CNT array made of CNTs with their length of 1 μm. However, the critical forces inducing the friction in CNT arrays composed of CNTs with their lengths of 5 and 10 μm are estimated as $F_{cr} = \sim 7$ and $\sim 0.2 \mu\text{N}$, respectively, which are smaller than the applied force (i.e. $F_{app} = 25 \mu\text{N}$). This indicates that the compression of CNT arrays consisting of CNTs with their lengths of 5 or 10 μm in response to an

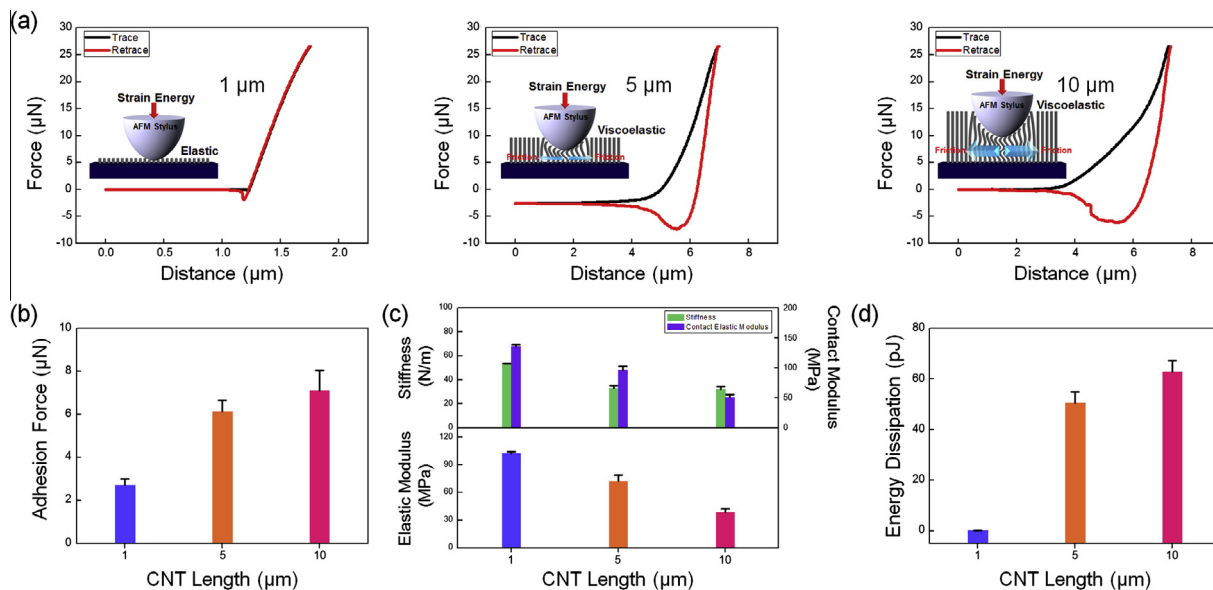


Fig. 2 – Nanomechanical properties of aligned CNT array measured in air. (a) Left panel shows the force–displacement curve of CNT array with CNT length of 1 μm, while middle panel indicates the force–displacement curve of CNT array with CNT length of 5 μm, while right panel provides the force–displacement curve of CNT array with CNT length of 10 μm. Nanomechanical properties for CNT array as a function of the length. (b) Adhesion forces, (c) stiffness, contact modulus, elastic modulus and (d) dissipated energies. (A colour version of this figure can be viewed online.)

applied force of 25 μN results in the viscoelastic behavior of CNT array due to the buckling-driven friction between CNTs during the compression.

For quantitative understanding of the mechanical behavior of CNT array, we have computed the elastic modulus of CNT array as a function of CNT length. In particular, the contact stiffness (S_c) is defined as the slope of an unloading curve at an applied force, i.e. $S_c = F_U/u|_{u=u_0}$, where F_U indicates a force measured along the unloading curve, u is the displacement, and u_0 is the indented displacement of CNT array that is compressed by an applied force F_{app} . The contact modulus (E_c) of CNT array can be obtained as [11]

$$E_c = \frac{(1 - \nu^2 S_c)}{2} \sqrt{\frac{\pi}{A_c}} \quad (1)$$

where ν is the Poisson's ratio of CNT array, and A_c is the contact area given by

$$A_c = \pi h_c^2 \tan^2 \theta \quad (2)$$

here, θ is the angle of an indenter (i.e. AFM tip), and h_c is the contact depth defined as

$$h_c = u_0 - \gamma F_{app} S_c^{-1} \quad (3)$$

where γ is a tip-dependent geometry parameter; in the AFM tip (i.e. conical tip), we have $\gamma = 0.72$. Based on the contact stiffness given by Eq. (1), we can calculate the elastic modulus of CNT array from a relation of [22]

$$E_c = \left[\frac{1 - \nu^2}{E} + \frac{1 - \nu_{tip}^2}{E_{tip}} \right]^{-1} \quad (4)$$

Here, E_{tip} and ν_{tip} represent the elastic modulus and Poisson's ratio of AFM tip, respectively, and E is the elastic modulus of CNT array. It is clearly shown in Fig. 2c that the elastic

modulus of CNT array depends on the structural parameter of CNT array (i.e. CNT length) such that as CNT length decreases, the contact modulus of CNT array increases. Moreover, in order to gain a quantitative insight into the viscoelastic behavior of CNT array, we have measured the dissipated energy during loading–unloading process for CNT array. The dissipated energy (W_D) is defined as:

$$W_D = \int_0^{u_0} [F_L(u) - F_U(u)] du \quad (5)$$

Here, F_L and F_U indicate the forces measured during loading and unloading processes, respectively. It is shown that the dissipated energy of CNT array composed of CNTs with their length of 1 μm is measured as <1 pJ, which indicates that the CNT array with CNT length of 1 μm exhibits the elastic properties. However, the dissipated energy of CNT array consisting of CNTs with their length of 5 μm (or 10 μm) is estimated as ~50 pJ (or ~65 pJ), which suggests that such CNT array possesses the viscoelastic properties due to friction between CNTs. Our observations provide that the structural parameter of CNT array (e.g. CNT length) determines whether CNT array exhibits the elastic or viscoelastic properties. This suggests that the ability of CNT array to serve as an energy absorbing material is determined from the structural parameters of CNT array.

3.2. Effect of solution surrounding CNT array on its mechanical properties

We have studied the effect of water on the mechanical properties of CNT array, which is attributed to our conjecture that water may mediate the indentation-driven frictional interactions between individual CNTs constituting the CNT array.

Here, it should be noted that since CNT possesses the superhydrophobic surface, it is usually difficult to fully wet the CNT array by dropping the water onto CNT array. In order to induce the wetting of CNT array, we have fully immersed the CNT array into the water for a sufficiently long time. When the CNT array is barely wetted, the effect of water on the mechanical behavior of CNT array may not be predominant, so that the mechanical deformation of barely wetted CNT array would be close to that of CNT array in normal air. This implies that the wetting behavior of CNT array may affect the mechanical (i.e. viscoelastic) properties of CNT array. In this work, in order to minimize the effect of wetting behavior of CNT array, we attempt to fairly wet the CNT array by immersing it to the water for a long time.

Fig. 3 depicts that the adhesion force, contact stiffness (or equivalently, contact modulus), and energy dissipation of CNT array, which consists of CNTs with their length of $1\ \mu\text{m}$, are not significantly affected by hydration. This independence of the mechanical properties of CNT array composed of short CNTs on hydration (i.e. water) can be easily understood from

our previous finding (e.g. Fig. 2a) that the mechanical behavior of such CNT array is determined from only elastic deformation of individual short CNTs without any frictional interactions between short CNTs. However, as anticipated, the mechanical properties of CNT array consisting of long CNTs (with their length of 5 or $10\ \mu\text{m}$) are critically dependent on hydration. In particular, water decreases the adhesion force of CNT array composed of long CNTs (Fig. 3a), while hydration increases the contact stiffness of such CNT array (Fig. 3b). It is found that hydration reduces the dissipated energy of CNT array consisting of long CNTs during loading–unloading process (Fig. 3c). This clearly suggests that water can mediate the indentation-driven frictional interactions between long CNTs that constitute the CNT array. That is, water can play a role in transition from the viscoelastic properties of CNT array (composed of long CNTs) to its elastic properties. Moreover, the dependence of the mechanical properties of CNT array on hydration is significantly governed by the length of CNTs comprising the CNT array. The longer CNTs constituting the CNT array, the larger change in mechanical properties (i.e.

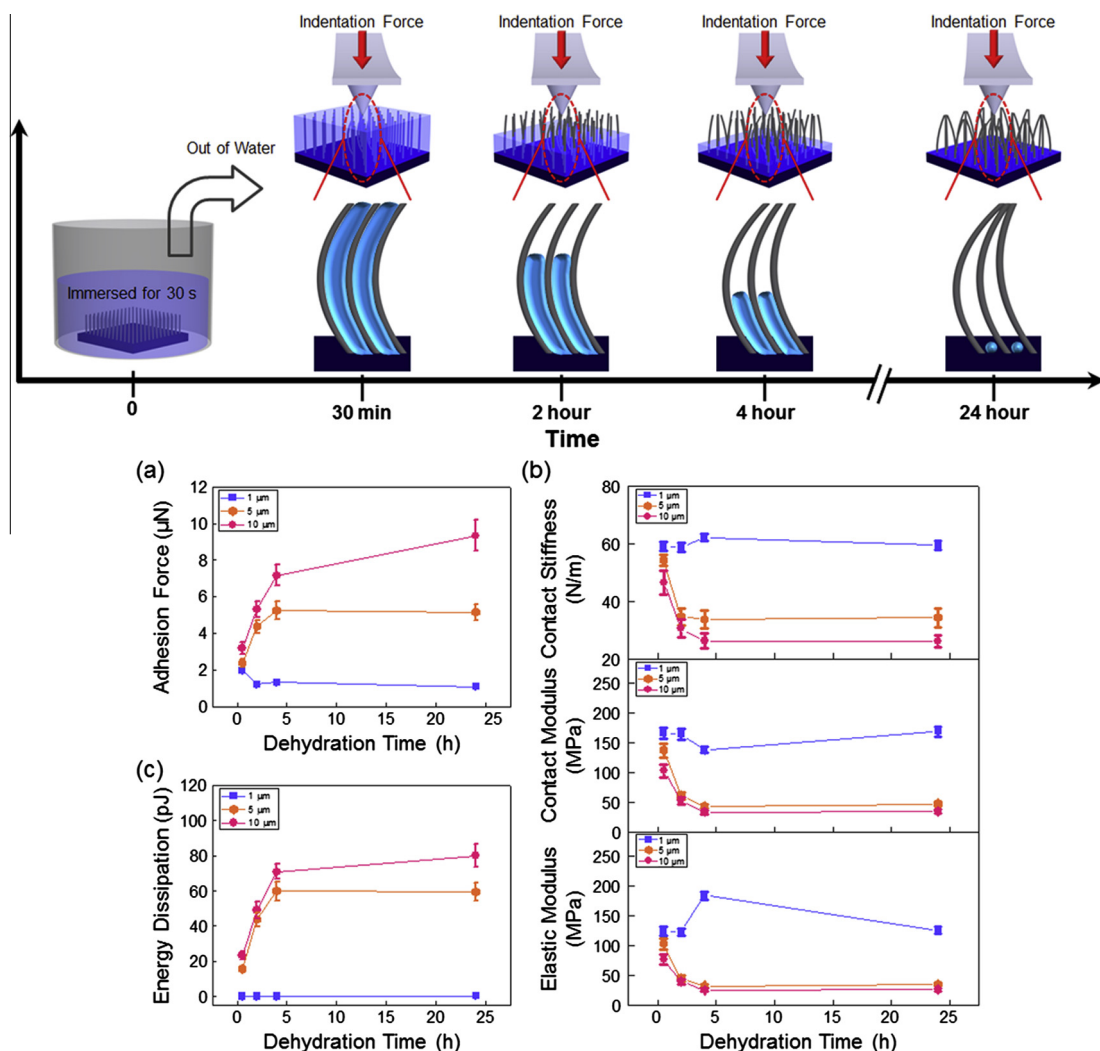


Fig. 3 – The changes of nanomechanical properties of aligned CNT array due to water. (a) Adhesion force, (b) contact stiffness, contact modulus, elastic modulus, and (c) dissipated energy, respectively, for CNT array, which was hydrated by water, as a function of dehydration time. (A colour version of this figure can be viewed online.)

adhesion force, contact modulus, and energy dissipation) for the CNT array (Fig. 3) due to water. This can be elucidated from our finding that longer CNTs constituting CNT array are more likely to induce the viscoelastic properties of the CNT array, and that hydration results in the transformation of the viscoelastic behavior of CNT array to its elastic behavior; the change of the mechanical properties of CNT array due to hydration (i.e. water molecules) is ascribed to the water-mediated transition from the viscoelastic behavior of CNT array into its elastic behavior. Since the length of CNTs constituting CNT array governs the viscoelastic behavior of the CNT array, the CNT length plays a role in the water-mediated transition from the viscoelastic behavior of CNT array to its elastic behavior. Furthermore, a change in the mechanical properties of CNT array is also dependent on the dehydration time (Fig. 3). This suggests that removal of water molecules allow the CNT array to recover its viscoelastic behavior from water-driven elastic behavior for CNT array. Our finding implies that not only the hydration level but also the structural parameter of CNT array determines the viscoelastic properties (i.e. contact modulus and energy dissipation) of CNT array.

We have also investigated the effect of hydrophobic solution such as decane solution on the mechanical properties of CNT array, which is ascribed to our conjecture that the different types of solution may induce the different frictional interactions between CNTs resulting in the different mechanical deformation behavior of CNT array. It is shown that the immersion of CNT array into decane solution significantly decreases the adhesion force of CNT array (Fig. 4a), whereas decane solution increases the contact stiffness of CNT array composed of long CNTs in comparison with that of CNT array in air (Fig. 4b). More remarkably, it is found that decane solution reduces the dissipated energy of CNT array during loading-unloading process. Moreover, the exposure of decane solution-immersed CNT array to air for 24 h does not allow the CNT array to recover the viscoelastic properties (i.e. energy dissipation) of CNT array (Fig. 4c). This elucidates that decane solution induces the different frictional interactions between CNTs (constituting CNT array) from the case of water-mediated frictional interaction between CNTs. In particular, the amount of reduction in the energy dissipation of CNT array (consisting of long CNTs) due to decane solution is larger than that due to water solution; this indicates that decane solution is more able to significantly induce the transition from the viscoelastic behavior of CNT array into its elastic behavior than water molecules is.

3.3. Microstructure analysis: solution-driven assembly of CNTs

In order to further gain insight into the solution-mediated frictional interaction between CNTs, which plays a role in the mechanical properties of CNT array, we consider the microstructure analysis using electron microscope images. Fig. 5a–c shows that CNT array consisting of short CNTs (i.e. with their length of 1 μm) remains nearly intact due to solution such as water and decane. However, both water and decane solutions induce a great change in the overall morphology of CNT array composed of long CNTs (i.e. with

their length of 10 μm) such that individual long CNTs are assembled by such solutions. We conjecture that there is a critical CNT length scale, at which a significant morphology change of CNT array due to solution-driven assembly process initiates. This assembly process dependent on the CNT length is probably due to the CNT length-dependent flexibility of CNT array [26]. This capillary-driven assembly due to water is found to play a major role on the mechanical properties of CNT array [8,27]. For example, when CNT array composed of long CNTs was hydrated by water, it induces the repulsion between CNTs, resulting in the decrease of mechanical friction between individual CNTs leading to a decrease in the energy dissipation of CNT array. On the other hand, the dehydration of CNT array beyond certain duration (e.g. 25 h) reduces the water-driven repulsion between CNTs (Fig. 5e). This process would restore and even further increase in the energy dissipation of CNT array. Similarly, for the decane-treated CNT array, the capillary-driven assembly was found for the CNT array composed of long CNTs (Fig. 5f). In particular, a recent study [28] reports that, based on molecular dynamics simulation, when decane molecules are adsorbed onto the surface of CNTs, the stability of CNT array increases. It is attributed to the fact that the decane molecule onto the CNT surface still remains and serves as a “glue” between CNTs in the array even after a sufficient dehydration. This result seems to be different from the case of water, where the water molecules would be completely evaporated during the dehydration process. It is presumed that the effective energy dissipation for the decane-treated CNT array is difficult to happen because the assembled array would behave as a large body during dehydration, which prevents an efficient recovery of viscoelastic properties of CNT array. The effect of hydration and subsequent dehydration is further examined by TEM analysis (Fig. 5g–i). A part of CNT array made of long CNTs without any treatment before AFM indentation experiment is shown in Fig. 5g. The CNTs are aggregated in the array and the average inner- and outer-diameters of such CNTs are found to be 9 and 14 nm, respectively. Upon water treatment the degree of aggregation of individual CNTs is found to increase (Fig. 5h), which is a good agreement with SEM result (Fig. 5e). The individual CNTs after decane treatment are found to stick together (Fig. 5i), which is possibly due to the adhesive interaction between the decane molecules and CNTs. The microstructure of CNT array is damaged during repeated AFM indentation experiment (inset of Fig. 5h).

4. Discussion: optimizing the damping properties

To gain a fundamental insight into the design principles providing how to optimize the energy dissipation of CNT array, we have introduced the dimensionless energy dissipation, which is useful in comparison between energy dissipations obtained from nanoscale experiment (e.g. nano-indentation) and macroscopic experiment (e.g. conventional tension/compression test). The dimensionless energy dissipation is defined as

$$\bar{W}_D = \frac{W_D}{W_E} = \frac{\int_0^{u_0} [F_L(u) - F_U(u)] du}{\int_0^{u_0} F_L(u) du} \quad (6)$$

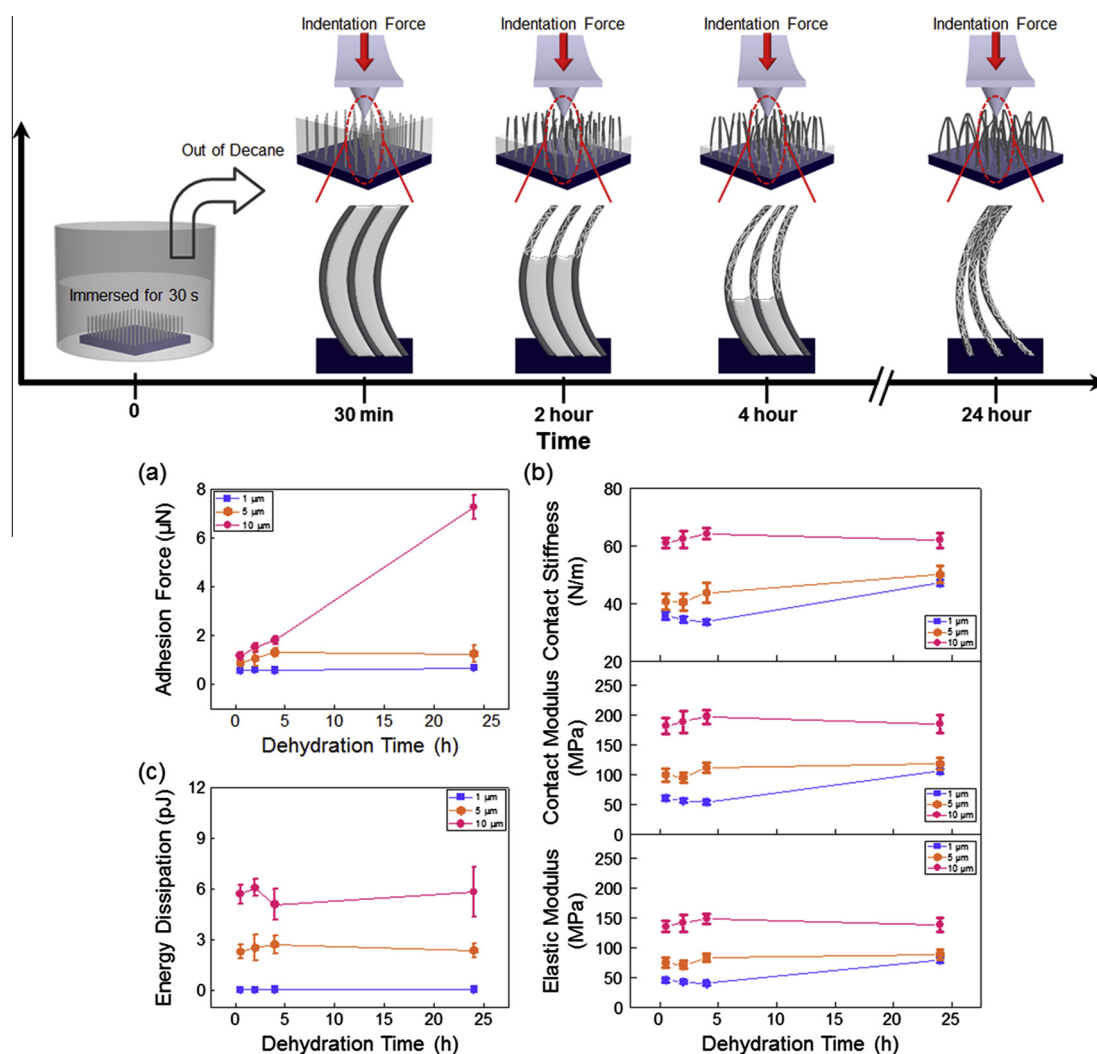


Fig. 4 – The changes of nanomechanical properties of aligned CNT array due to decane solution. (a) Adhesion force, (b) contact stiffness, contact modulus, elastic modulus, and (c) dissipated energy, respectively, for CNT array, which was hydrated by hydrophobic solution, as a function of dehydration time. (A colour version of this figure can be viewed online.)

where W_D is the dissipated energy during loading–unloading process, which can be computed from Eq. (5), and W_E is the stored elastic energy during the loading process. Fig. 6 provides the dimensionless energy dissipation of CNT array as a function of CNT length and the type of medium surrounding CNTs constituting a CNT array (see also Table 1). It is shown that the dissipated energy of CNT array consisting of short CNTs during loading–unloading process is in the order of 1% (with respect to the stored strain energy), which indicates that such a CNT array behaves as an elastic material, whereas the mechanical process leads CNT array composed of long CNTs to dissipate the energy in a range of 60%, which suggests that such a CNT array can serve as a mechanical damper (or shock absorbing material). This clearly elucidates the role of CNT length on the ability of CNT array to dissipate the energy during loading–unloading process. Specifically, the CNT length scale determines the deformation mechanism of CNT array (Table 1); when the array made of short CNTs is deformed by a force, the CNT array undergoes the elastic deformation. On the other hand, for CNT array made of long CNTs,

the CNT array experiences the viscoelastic deformation mechanism due to force-driven buckling of nanotubes (that induces the friction between nanotubes). It is remarkably found that the dimensionless dissipated energy of CNT array consisting of CNTs with their length of 10 µm is higher than that of Kevlar (Ref. [29]), which is one of polymers that perform excellent mechanical function (e.g. mechanical damping), and other polymers, e.g. polypropylene and acrylic (Ref. [30]). This indicates that the CNT array is able to perform the remarkable mechanical damping better than polymeric materials. Moreover, as shown in Fig. 6, a chemical environment surrounding CNTs constituting the CNT array plays a role in the mechanical behavior of CNT array. Specifically, it is found that decane solution is more useful in decreasing the energy dissipation of CNT array than water molecule. In other words, decane solution is suitable to induce the transition of the viscoelastic property of CNT array into its elastic property. Moreover, upon evaporation of decane solution (>24 h), the viscoelastic property of CNT array is not recovered, which is attributed to the fact that decane molecules

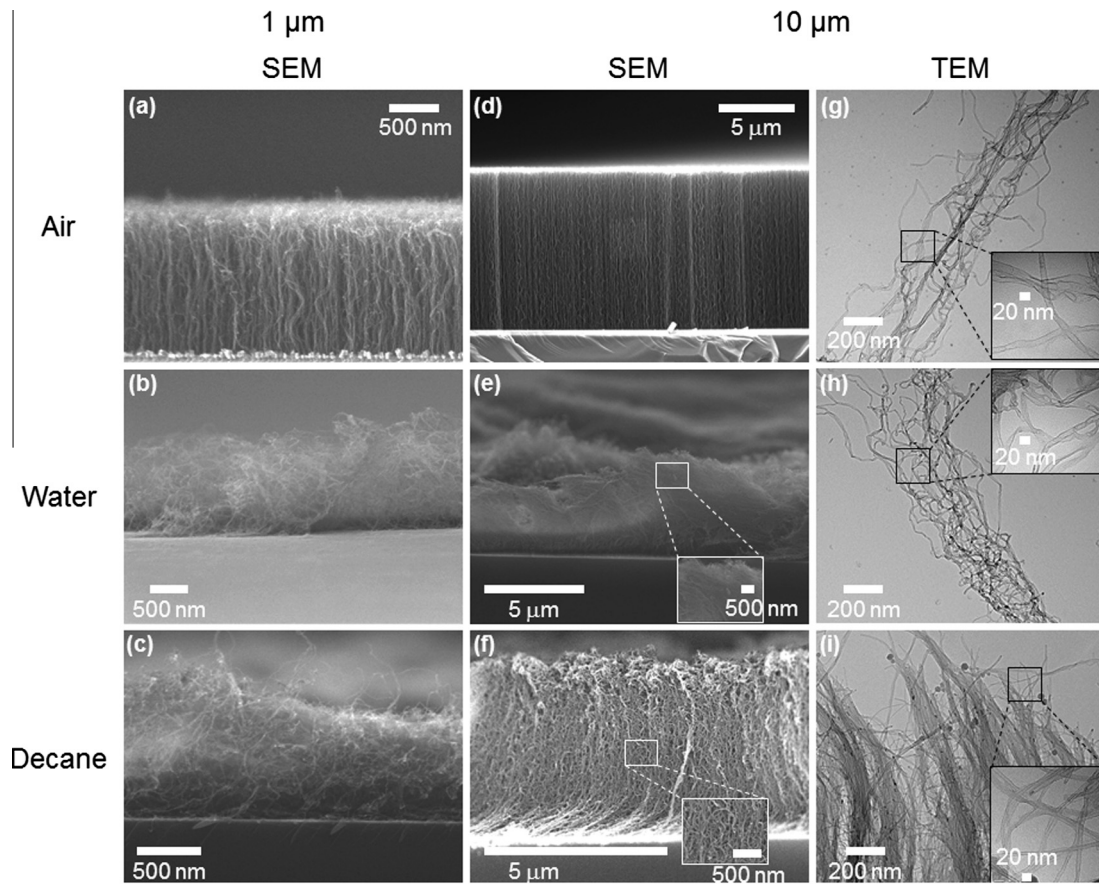


Fig. 5 – Electron microscope images of CNT array. SEM images for CNT array with CNT length of 1 μm (a) without any treatment, and treated (b) with water or (c) decane solution. SEM images for CNT array with CNT length of 10 μm (d) without any treatment, and treated with (e) water or (f) decane solution. TEM images for CNT array with CNT length of 10 μm (g) without any treatment, and treated with (h) water or (i) decane solution. AFM indentation experiments were not carried out for only (a), (d), and (g). Each inset shows the enlarged images of CNTs comprising the CNT array. Inset figures in (e), (h), (f), and (i) depict the assembled CNTs due to solution (e.g. water and decane).

are still adsorbed onto the surface of CNTs even when decane solution is evaporated. On the other hand, when the CNT array immersed into water is dehydrated (>24 h), the viscoelastic behavior of CNT array is recovered, which suggests that water molecules attached to the surface of CNTs are completely removed upon dehydration. This may suggest that the immersion of CNT array into medium (or evaporation of medium) affects the adhesive and frictional interactions between CNTs, which eventually makes an effect on the viscoelastic behavior of CNT array. In summary, as described in Fig. 6, the key design parameters that determines the deformation mechanism of CNT array, are the CNT length and chemical environment surrounding CNTs. To improve the viscoelastic behavior of CNT array, we need to understand the mechanistic origin of the viscoelastic behavior of CNT array. If one is able to change the mechanistic deformation mechanism of CNT array, then the mechanical (viscoelastic) properties of CNT array would be manipulated. As described in Section 3.1, the viscoelastic behavior of CNT array is attributed to the buckling-driven friction between CNTs constituting CNT array. The viscoelastic behavior of CNT array may be tunable by changing the CNT alignment that affects the

interaction between CNTs as described in a literature [31]. Moreover, the viscoelastic behavior of CNT array is also related to the adhesive interactions between CNTs. Specifically, Zhou et al. [32] showed that the adhesive interaction affects the topology of both CNT and CNT array. More interestingly, a recent study [33] reports that, by using molecular dynamics simulation, the adhesive interactions between CNTs make an impact on the mechanical deformation of CNT array. This may be consistent with our finding (e.g. Fig. 5) that the viscoelastic behavior of CNT array critically depends on the type of medium, which makes an effect on adhesive interactions between CNTs. In addition, as described in a literature [34], the viscoelastic behavior of CNT array may be also affected by buckling that leads to separation of bundled CNTs.

One of possible routes to improve the viscoelastic behavior of CNT array by changing its deformation mechanism, is to chemically functionalize CNTs (e.g. using DNA molecules [35]), which will affect both frictional and adhesive interactions between CNTs; this chemical functionalization of CNTs will result in the tunable viscoelastic behavior of CNT array depending on the level of chemical functionalization. Moreover, the chemical functionalization is also able to induce

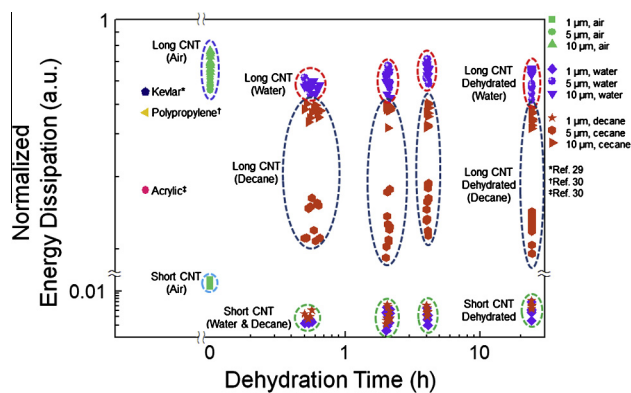


Fig. 6 – Dimensionless energy dissipations of aligned CNT array and polymers. Dimensionless energy dissipations of Kevlar (Ref. [29], navy symbol), Polypropylene (Ref. [30], yellow symbol), and Acrylic (Ref. [30], pink symbol) are calculated by digitized method based on the force-distance curve. Green symbols indicate the energy dissipation of aligned CNT array in air. Purple symbols represent the energy dissipation of aligned CNT array due to water. Orange symbols provide the energy dissipation of aligned CNT array in decane solution. Here, CNT array is composed of short CNT (with their length of 1 μm) or long CNTs (with their length of 5 μm , or 10 μm). (A colour version of this figure can be viewed online.)

the bundling of CNTs, which leads to the different deformation mechanism of CNT array. A recent molecular dynamics simulation found that the high mechanical strength of carbon fiber is attributed to the fact that friction between chiral CNTs in a hexagonally closed packed bundle is sufficient to exert huge interaction forces between CNTs constituting the carbon fiber [36]. Another route to enhance the viscoelastic behavior of CNT array is to change the inter-spacing distance between CNTs constituting the CNT array, which eventually affects the porosity of CNT array. A recent study by Cranford and Buehler [33] reports that the porosity of the film made of CNTs is a key design parameter that determines the mechanical deformation mechanism of CNT-based films and membranes. This suggests that it is possible to improve the energy dissipation of CNT array by controlling the porosity of CNT array.

Moreover, since the deformation mechanism of CNT array depends on the loading mode (i.e. how a mechanical force is applied), the viscoelastic behavior of CNT array may be affected by the loading mode. In this work, the deformation mechanism of CNT array is due to a force that is applied in a direction parallel to the longitudinal direction of CNT (i.e. along the CNT length). If a mechanical force is applied perpendicular to the longitudinal direction of CNT as in a case of CNT buckypaper [33], the deformation mechanism of CNT array may be mostly attributed to the bending of individual CNTs as well as adhesive interactions between CNTs. This implies that the mechanical deformation mechanism of CNT array is significantly affected by the loading direction, suggesting that the viscoelastic properties (i.e. energy dissipation) of CNT array are critically dependent on the loading mode.

Table 1 – Energy dissipation mechanism of CNT array at multiple length scale.

Solution type	CNT length scale (μm)	Energy dissipation (pJ)	Deformation mechanism
Air	1	<0.1	Elastic behavior
	5	~ 50	Viscoelastic behavior
	10	~ 70	Viscoelastic behavior
Water	1	<0.1	Elastic behavior
	5	~ 3	Viscoelastic behavior
	10	~ 6	Viscoelastic behavior
Decane	1	<0.1	Elastic behavior
	5	20–60	Viscoelastic behavior
	10	20–70	Viscoelastic behavior

5. Conclusions

In this work, we have demonstrated the design principles showing how to modulate the mechanical properties of CNT array that can serve as an energy-absorbing material as can do a cellular material. The mechanical properties of CNT array can be controllable by tailoring the indentation-driven frictional interaction between CNTs, which depends on both the structural parameter of CNT array and the solution that mediates the interaction between CNTs. This shows how to effectively design the CNT array that can perform the energy adsorption. In the broader context, this approach is based on the hypothesis that interaction between CNTs constituting CNT array can be manipulated through appropriately changing a chemical environment around them. Similarity can be found in a previous study [35] reporting that enzyme mediates a degree of aggregation of DNA functionalized CNTs. The fundamental principles for our work regarding the solution-mediated mechanical properties of CNT array is not fully understood at this present stage. However, it is noteworthy enough that the result demonstrated here would provide a further insight into the design principles for CNT-based structure, as a foam-like material, which can perform the function of energy adsorption for future applications in engineering, military, nanoscience and nanotechnology. Further efforts should afford proof that interfaces the controllable mechanical properties of CNT-based mechanical devices such as biomimetic muscle units and mechanical energy storage system.

Acknowledgements

T.K. appreciates the financial support from National Research Foundation of Korea (NRF) under Grant Nos. 2012R1A1B3002706 and 2012R1A2A2A04047240. K.E. gratefully acknowledges the financial support from NRF under Grant No. NRF-2012R1A1A2008616. J.-H.H. appreciates the financial support from NRF under Grant No. NRF-2012R1A1A1015734 and Agency for Defense Development through Chemical and Biological Defense Research Center.

Appendix A. Supplementary data

Supplementary data associated with this article can be found, in the online version, at <http://dx.doi.org/10.1016/j.carbon.2013.08.030>.

REFERENCES

- [1] Dai H. Carbon nanotubes: synthesis, integration, and properties. *Acc Chem Res* 2002;35(12):1035–44.
- [2] Han J-H, Paulus GLC, Maruyama R, Heller DA, Kim W-J, Barone PW, et al. Exciton antennas and concentrators from core-shell and corrugated carbon nanotube filaments of homogeneous composition. *Nat Mater* 2010;9(10):833–9.
- [3] Eom K, Park HS, Yoon DS, Kwon T. Nanomechanical resonators and their applications in biological/chemical detection: nanomechanics principles. *Phys Rep* 2011;503(3–4):115–63.
- [4] Wong EW, Sheehan PE, Lieber CM. Nanobeam mechanics: elasticity, strength, and toughness of nanorods and nanotubes. *Science* 1997;277(5334):1971–5.
- [5] Lu JP. Elastic properties of carbon nanotubes and nanoropes. *Phys Rev Lett* 1997;79(7):1297.
- [6] Cao A, Dickrell PL, Sawyer WG, Ghasemi-Nejhad MN, Ajayan PM. Super-compressible foamlike carbon nanotube films. *Science* 2005;310(5752):1307–10.
- [7] Suhr J, Victor P, Ci L, Sreekala S, Zhang X, Nalamasu O, et al. Fatigue resistance of aligned carbon nanotube arrays under cyclic compression. *Nat Nanotechnol* 2007;2(7):417–21.
- [8] Chakrapani N, Wei B, Carrillo A, Ajayan PM, Kane RS. Capillarity-driven assembly of two-dimensional cellular carbon nanotube foams. *Proc Natl Acad Sci USA* 2004;101(12):4009–12.
- [9] Pushparaj VL, Shaijumon MM, Kumar A, Murugesan S, Ci L, Vajtai R, et al. Flexible energy storage devices based on nanocomposite paper. *Proc Natl Acad Sci USA* 2007;104(34):13574–7.
- [10] Teo EHT, Yung WKP, Chua DHC, Tay BK. A carbon nanomattress: a new nanosystem with intrinsic, tunable damping properties. *Adv Mater* 2007;19(19):2941–5.
- [11] Gouldstone A, Chollacoop N, Dao M, Li J, Minor AM, Shen Y-L. Indentation across size scales and disciplines: recent developments in experimentation and modeling. *Acta Mater* 2007;55(12):4015–39.
- [12] Dickinson ME, Schirer JP. Probing more than the surface. *Mater Today* 2009;12(7–8):46–50.
- [13] Roos WH, Bruinsma R, Wuite GJL. Physical virology. *Nat Phys* 2010;6(10):733–43.
- [14] Suresh S. Biomechanics and biophysics of cancer cells. *Acta Mater* 2007;55(12):3989–4014.
- [15] Palaci I, Fedrigo S, Brune H, Klinke C, Chen M, Riedo E. Radial elasticity of multiwalled carbon nanotubes. *Phys Rev Lett* 2005;94(17):175502.
- [16] Barboza APM, Chacham H, Neves BRA. Universal response of single-wall carbon nanotubes to radial compression. *Phys Rev Lett* 2009;102(2):025501.
- [17] Sohn Y-S, Park J, Yoon G, Jee S-W, Lee J-H, Na S, et al. Mechanical properties of silicon nanowires. *Nanoscale Res Lett* 2010;5(4):211–6.
- [18] Li X, Gao H, Murphy CJ, Caswell KK. Nanoindentation of silver nanowires. *Nano Lett* 2003;3(11):1495–8.
- [19] Wang Z, Mook WM, Niederberger C, Ghisleni R, Philippe L, Michler J. Compression of nanowires using a flat indenter: diametrical elasticity measurement. *Nano Lett* 2012;12(5):2289–93.
- [20] Song C, Kwon T, Han J-H, Shandell M, Strano MS. Controllable synthesis of single-walled carbon nanotube framework membranes and capsules. *Nano Lett* 2009;9(12):4279–84.
- [21] Hall LJ, Coluci VR, Galvão DS, Kozlov ME, Zhang M, Dantas SO, et al. Sign change of Poisson's ratio for carbon nanotube sheets. *Science* 2008;320(5875):504–7.
- [22] Johnson KL. Contact mechanics. Cambridge University Press; 1987.
- [23] Oliver WC, Pharr GM. An improved technique for determining hardness and elastic modulus using load and displacement sensing indentation experiments. *J Mater Res* 1992;7(6):1564–83.
- [24] Han J-H, Graff RA, Welch B, Marsh CP, Franks R, Strano MS. A mechanochemical model of growth termination in vertical carbon nanotube forests. *ACS Nano* 2008;2(1):53–60.
- [25] Gere JM. Mechanics of materials. 6th ed. Thomson Learning; 2003.
- [26] Lau KKS, Bico J, Teo KBK, Chhowalla M, Amaratunga GAJ, Milne WI, et al. Superhydrophobic carbon nanotube forests. *Nano Lett* 2003;3(12):1701–5.
- [27] Wirth CT, Hofmann S, Robertson J. Surface properties of vertically aligned carbon nanotube arrays. *Diam Relat Mater* 2008;17(7–10):1518–24.
- [28] Wei C. Adsorption of an alkane mixture on carbon nanotubes: selectivity and kinetics. *Phys Rev B* 2009;80(8):85409.
- [29] Graham JF, McCague C, Warren OL, Norton PR. Spatially resolved nanomechanical properties of Kevlar fibers. *Polymer* 2000;41(12):4761–4.
- [30] Chalivendra V, Calvert P, Wanasekara N. Nanoscale surface embrittlement of fibers. National Textile Center; 2008.
- [31] Girifalco LA, Hodak M, Lee RS. Carbon nanotubes, buckyballs, ropes, and a universal graphitic potential. *Phys Rev B* 2000;62(19):13104.
- [32] Zhou W, Huang Y, Liu B, Hwang KC, Zuo JM, Buehler MJ, et al. Self-folding of single- and multiwall carbon nanotubes. *Appl Phys Lett* 2007;90(7):73107.
- [33] Cranford SW, Buehler MJ. *In silico* assembly and nanomechanical characterization of carbon nanotube buckypaper. *Nanotechnology* 2010;21(26):265706.
- [34] Volkov AN, Zhigilei LV. Structural stability of carbon nanotube films: the role of bending buckling. *ACS Nano* 2010;4(10):6187–95.
- [35] Arnett CM, Marsh CP, Welch CR, Strano MS, Han J-H, Gray JH, et al. Enzyme-mediated assimilation of DNA-functionalized single-walled carbon nanotubes. *Langmuir* 2009;26(2):613–7.
- [36] Majure DL, Haskins RW, Lee NJ, Welch CR, Cornwell CF. Simulations of simple nanomachines in carbon nanotube bundles based on chirality. US Army Engineer Research and Development Center; 2008.

Electronic Supplementary Material

Controllable viscoelastic behavior of vertically aligned carbon nanotube array

Kilho Eom¹, Kihwan Nam², Huihun Jung², Pilhan Kim³, Michael S. Strano⁴, Jae-Hee Han^{5,*}, and Taeyun Kwon^{3,*}

¹Biomechanics Laboratory, College of Sport Science, Sungkyunkwan University, Suwon, 440-746, Republic of Korea

²Department of Biomedical Engineering, Yonsei University, Wonju, 220-710, Republic of Korea

³Graduate School of Nanoscience and Technology, Korea Advanced Institute of Science and Technology (KAIST), Daejeon 305-701, Republic of Korea

⁴Department of Chemical Engineering, Massachusetts Institute of Technology, Cambridge, Massachusetts 02139, USA,

⁵Department of Energy IT, Gachon University, Gyeonggi-do, 461-701, Republic of Korea

*Correspondence should be addressed to J.-H. H. (E-mail: jghan388@gachon.ac.kr) and T. K. (E-mail: taeyunkwon@kaist.ac.kr)

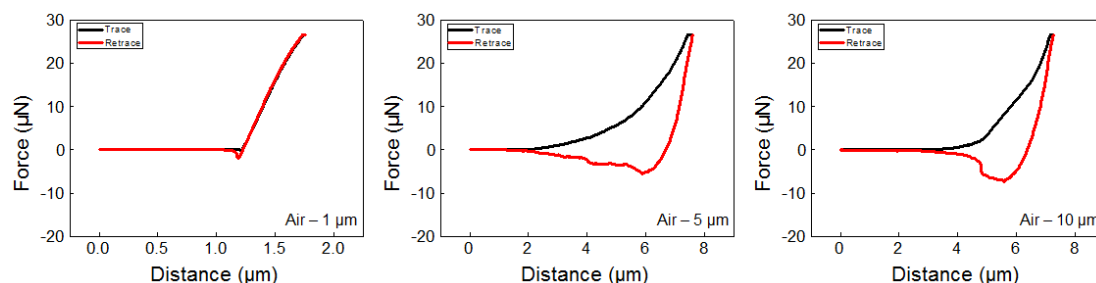


Figure S1. Force-distance curves of aligned CNT arrays measured in air. Left panel shows the force-displacement curve of aligned CNT array consisting of short CNTs with their length of 1 μm , while middle panel indicates the force-distance curve of aligned CNT array composed of CNTs with their length of 5 μm , while right panel provides the force-displacement curve of aligned CNT array made of CNTs with their length of 10 μm .

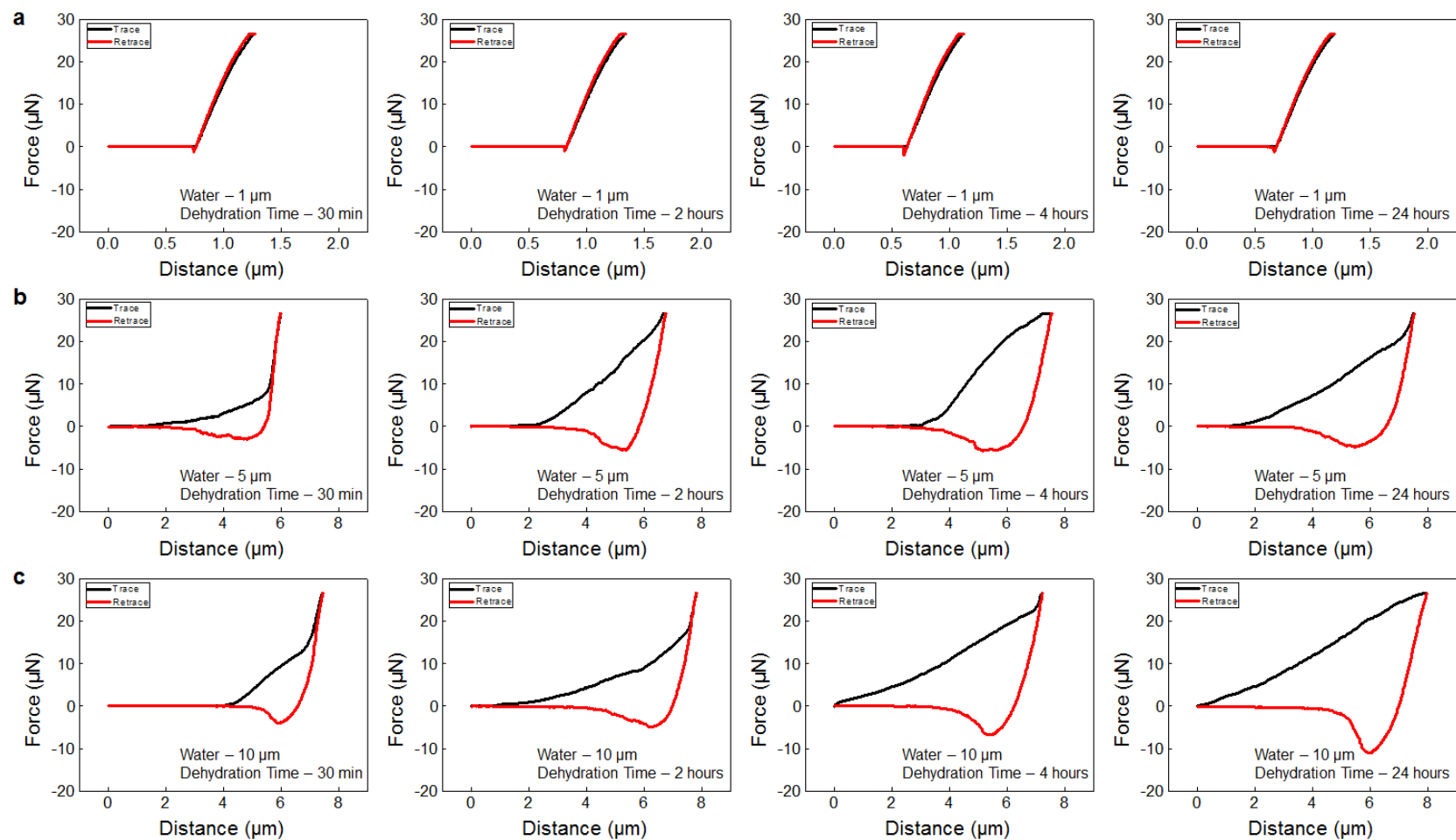


Figure S2. Force-distance curves of aligned CNT arrays immersed in water and subsequently dehydrated. (a) Force-distance curve of aligned CNT array consisting of short CNTs with their length of 1 μm. (b) Force-distance curves of aligned CNT array composed of CNTs with their length of 5 μm. (c) Force-distance curve of aligned CNT array made of CNTs with their length of 10 μm. Here, force-displacement curves were measured at dehydration time of 30 min (left), 2 hours (center left), 4 hours (center right), and 24 hours (right), respectively.

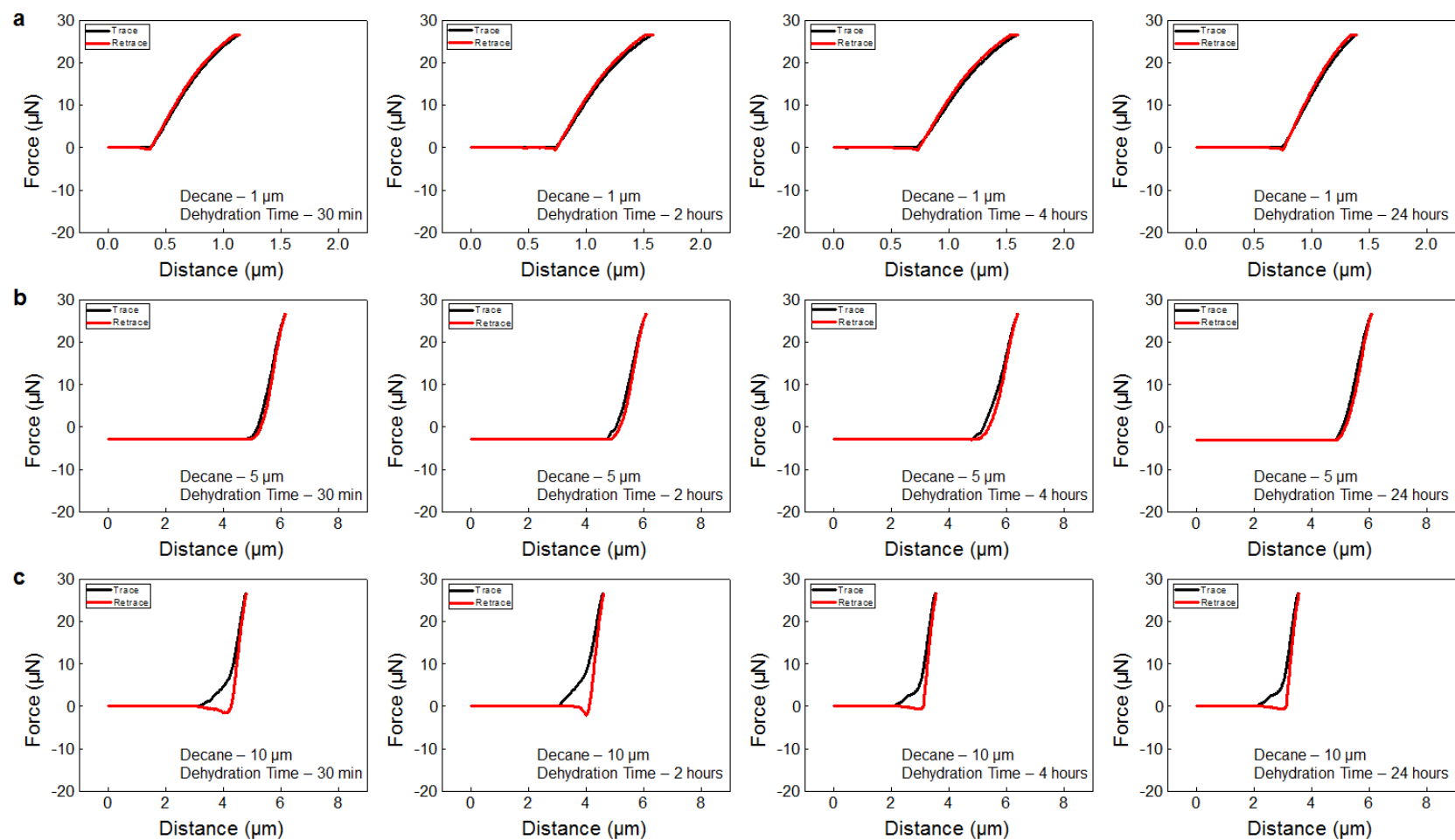


Figure S3. Force-distance curves of aligned CNT arrays immersed in decane solution and subsequently dehydrated. (a) Force-distance curve of aligned CNT array consisting of short CNTs with their length of 1 μm. (b) Force-distance curves of aligned CNT array composed of CNTs with their length of 5 μm. (c) Force-distance curve of aligned CNT array made of CNTs with their length of 10 μm. Here, force-displacement curves were measured at dehydration time of 30 min (left), 2 hours (center left), 4 hours (center right), and 24 hours (right), respectively.